AGU PUBLICATIONS

Geochemistry, Geophysics, Geosystems

RESEARCH ARTICLE
10.1002/2016GC006325

Key Points:
- Two different cleaning methods for downcore foraminiferal Mg/Ca analyses give significantly different results
- Shallow subsurface warming preceded by a decrease in seawater $\delta^{18}O$ during HS1
- Early Eemian characterized by relatively cold, high-salinity shallow-subsurface water

Supporting Information:
- Supporting Information S1

Correspondence to:
M. M. Ezat,
mohamed.ezat@uit.no

Citation:
Ezat, M. M., T. L. Rasmussen, and J. Groeneveld (2016), Reconstruction of hydrographic changes in the southern Norwegian Sea during the past 135 kyr and the impact of different foraminiferal Mg/Ca cleaning protocols, *Geochem. Geophys. Geosyst.*, *17*, doi:10.1002/2016GC006325.

Received 26 FEB 2016
Accepted 1 AUG 2016
Accepted article online 9 AUG 2016

Reconstruction of hydrographic changes in the southern Norwegian Sea during the past 135 kyr and the impact of different foraminiferal Mg/Ca cleaning protocols

Mohamed M. Ezat[1,2], Tine L. Rasmussen[1], and Jeroen Groeneveld[3]

[1]CAGE - Centre for Arctic Gas Hydrate, Environment and Climate, Department of Geology, UiT, Arctic University of Norway, Tromsø, Norway, [2]Department of Geology, Faculty of Science, Beni-Suef University, Beni-Suef, Egypt, [3]Center for Marine Environmental Sciences (MARUM), University of Bremen, Bremen, Germany

Abstract The shallow subsurface hydrography in the southern Norwegian Sea during the past 135,000 years was investigated using parallel measurements of Mg/Ca and $\delta^{18}O$ in shells of the planktic foraminiferal species *Neogloboquadrina pachyderma*. Two cleaning methods were applied prior to Mg/Ca analysis, "Mg cleaning" and "full cleaning" methods. Different results were obtained, which are most likely due to a more efficient removal of Mn-contaminant coatings of the shells, when the "full cleaning" procedure was applied. We further combined Mg/Ca and B/Ca from the "full cleaning" method with $\delta^{18}O$ values to constrain the calcification temperature and seawater-$\delta^{18}O$ ($\delta^{18}O_{sw}$) in the past. During Heinrich Stadial (HS)1 (~18.5–15 ka) *N. pachyderma* constituted >80% of the planktic foraminiferal population, $\delta^{18}O_{sw}$ decreased by ~1.5‰, and shallow subsurface temperature increased by ~1.5–3°C, suggesting strong stratification in the upper water column and a possible subsurface inflow of Atlantic water below a well-developed halocline during the calcification seasons of *N. pachyderma*. Similar decreases in $\delta^{18}O_{sw}$ are also recorded for other Heinrich stadials (HS2, 3, 4, 6, and 11). Our temperature estimates confirm previous observations of the delay of the last interglacial "Eemian" warm peak in the eastern Nordic Seas compared to the North Atlantic, and a late warming coinciding with the summer insolation minimum at 60°N. In addition, relatively high values of $\delta^{18}O_{sw}$ during the early Eemian suggest a shallow subsurface inflow of Atlantic water below a thin layer of Arctic surface water.

1. Introduction

Northeastward flow of Atlantic surface water across the Greenland-Scotland ridge into the Nordic Seas and Arctic Ocean releases heat to the atmosphere. The surface water is transformed to dense, cold deep water that overflows the Greenland-Scotland Ridge to the North Atlantic [e.g., *Hansen and Østerhus*, 2000; *Eldevik et al.*, 2009]. It has been suggested that an increase in ocean stratification in the high-latitude North Atlantic due to warming and addition of meltwater reduces the surface heat transport toward the Arctic and deep-water formation, affecting regional climate and the large-scale atmospheric circulation [e.g., *Drijfhout et al.*, 2015; *Rahmstorf et al.*, 2015]. Reconstruction of the history of Atlantic water inflow in connection with past climate change could provide better understanding of how ocean circulation in this area and climate are linked. Significant changes in the properties of Atlantic water inflow into the Nordic Seas during the past 150,000 years associated with past regional and global climate change were revealed based on planktic foraminiferal $\delta^{18}O$ and faunal assemblages [e.g., *Rasmussen et al.*, 1996; *Fronval and Jansen*, 1997; *Bauch et al.*, 2001].

Foraminiferal $\delta^{18}O$ values are a function of calcification temperature, seawater $\delta^{18}O$ ($\delta^{18}O_{SW}$), and carbonate chemistry [*Emiliani*, 1955; *Shackleton*, 1967; *Spero et al.*, 1997]. $\delta^{18}O_{SW}$ values at a specific location vary through time due to changes in global ice volume, evaporation/precipitation, meltwater and river runoff, and past changes in ocean circulation [*Craig*, 1961; *Dansgaard*, 1964; *Shackleton*, 1967; *Waelbroeck et al.*, 2011; *Friedrich and Timmermann*, 2012]. Differentiating between the various signals is a challenge, but imperative for our understanding of the temporal variability in foraminiferal $\delta^{18}O$. Minor/trace element to calcium ratios can provide independent information about the calcification temperature [e.g., *Nürnberg*, 1995; *Nürnberg et al.*, 1996], salinity-related effects [e.g., *Hönisch et al.*, 2011; *Bahr et al.*, 2013], and carbonate

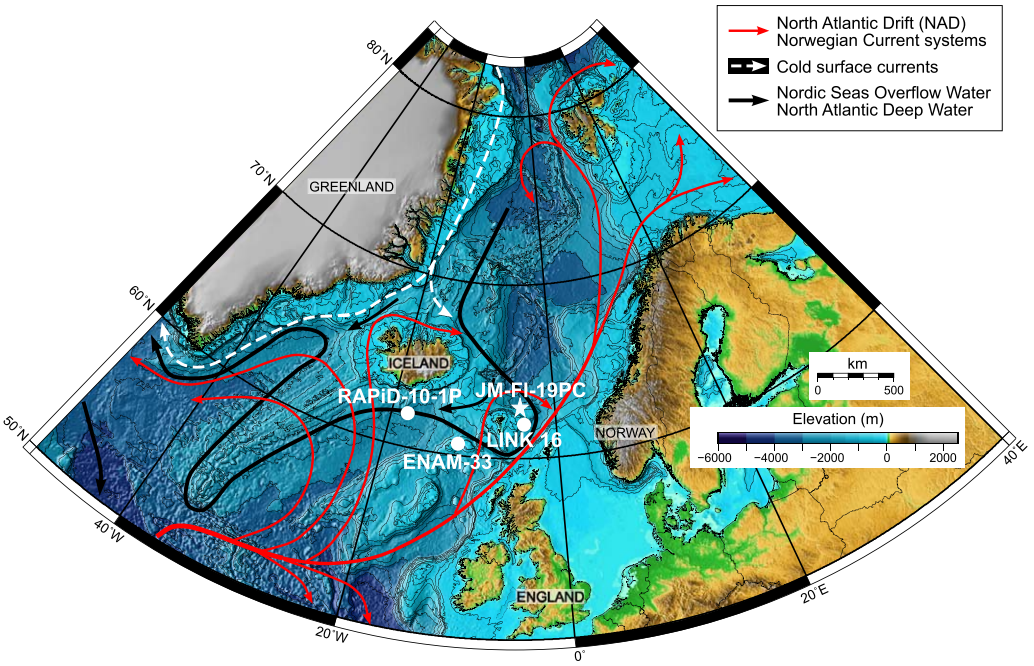

Figure 1. Map showing the major surface and bottom water currents in the northern North Atlantic and the Nordic Seas [*Hansen and Østerhus*, 2000; *Mork and Blindheim*, 2000; *Orvik and Niiler*, 2002; *Jakobsen et al*., 2003]. The location of investigated core JM11-FI-19PC is also indicated (white star). White circles refer to sediment cores ENAM-33 (1217 m water depth) [*Rasmussen et al*., 2003a], LINK 16 (773 m water depth) [*Abbott et al*., 2014], and RAPiD-10-1P (1237 m water depth) [*Thornalley et al*, 2010]. The map is modified after *Ezat et al*. [2014].

chemistry [e.g., *Yu et al*., 2007a]. In particular, Mg/Ca is widely used in parallel with δ^{18}O measurements to constrain calcification temperatures and $\delta^{18}O_{SW}$ [e.g., *Elderfield and Ganssen*, 2000; *Thornalley et al*., 2009]. In this study, we use parallel minor/trace element and δ^{18}O measurements in the planktic foraminiferal species *N. pachyderma* in order to reconstruct variability of the Atlantic water flow into the Nordic Seas for the last 135 kyr. The study is based on sediment core JM-FI-19PC, collected northwest of the Faroe Islands (62°49′N, 03°52′W; 1179 m water depth) [*Ezat et al*., 2014], where the largest Atlantic water inflow into the Nordic Seas takes place today (Figure 1) [*Hansen and Østerhus*, 2000]. The investigated time interval comprises the last 135 kyr, and includes the Holocene interglacial, the last glacial cycle, and the Eemian interglacial, which represent different climate boundary conditions. During the Eemian (∼135–115 ka), summer temperatures in the northern hemisphere were higher than in the Holocene period 10–0 kyr [*CAPE-Last Interglacial Project Members*, 2006]. Greenland ice cores have revealed rapid climatic changes from cold stadials to warm interstadials during the last glacial and deglaciation (∼110–10 ka), the so-called Dansgaard-Oeschger (DO) events [*Dansgaard et al*., 1993]. In North Atlantic and Nordic Seas sediments, DO events are associated with the deposition of Ice Rafted Debris (IRD). In the North Atlantic, 11 particularly prominent IRD layers rich in detrital carbonate originating from the Hudson Strait were recorded in the past 150 kyr [*Heinrich*, 1988; *Hemming*, 2004]. These events are called Heinrich events and are thought to correlate in time with the coldest periods of the longest lasting stadials in the ice cores [*Heinrich*, 1988; *Bond et al*., 1993; *Broecker*, 1994; *Rasmussen et al*., 2003b; *Hemming*, 2004, *Barker et al*., 2011]. The entire stadial period during which a Heinrich event is recorded is defined as a Heinrich Stadial (HS) [cf. *Barker et al*., 2009].

Large depletions in planktic δ^{18}O measured in *N. pachyderma* (0.5–2.5‰) were recorded during the stadial events in the Nordic Seas. Different interpretations have been proposed for these δ^{18}O depletions including increase in sea surface buoyancy [e.g., *Rasmussen et al*., 1996; *Stanford et al*., 2011], increased rate of sea ice formation [*Hillaire-Marcel and de Vernal*, 2008], and/or increase in temperature [e.g., *Petersen et al*., 2013]. Previous studies have also recorded changes in planktic δ^{18}O during the Eemian in the North Atlantic and Nordic Seas, but with much less amplitude and frequency [e.g., *Fronval and Jansen*, 1997; *Rasmussen et al*., 2003a; *Irvali et al*., 2012; *Galaasen et al*., 2014]. Parallel minor/trace element (in particular Mg/Ca) and δ^{18}O measurements in *N. pachyderma* can potentially decipher the causes of the δ^{18}O variations and hence

improve our understanding of past changes in the properties of the near-surface water and changes in ocean circulation in the Nordic Seas on DO and glacial-interglacial time scales. So far, no records of combined Mg/Ca and $\delta^{18}O$ exist for the SE Nordic Seas on these time scales.

Laboratory experiments have shown that temperature exerts a primary control on the incorporation of Mg into planktic foraminiferal $CaCO_3$, while other factors such as salinity and carbonate chemistry play a minor role [e.g., *Nürnberg et al*., 1996; *Russell et al*., 2004; *Hönisch et al*., 2013; *Spero et al*., 2015]. However, the primary Mg/Ca signal can be significantly modified by partial dissolution [e.g., *Dekens et al*., 2002; *Regenberg et al*., 2006], as well as contamination with organic material, adsorbed clays and postdepositional overgrowths [*Boyle*, 1981]. In order to remove different contaminants, three main procedures have been developed for preparing foraminiferal samples for minor/trace element analyses, the "Mg cleaning," "Cd cleaning," and "full cleaning" methods [*Boyle and Keigwin*, 1985; *Martin and Lea*, 2002; *Barker et al*., 2003; for review see *Barker et al*., 2005]. Compared to the "Mg cleaning," the "Cd cleaning" method includes an additional reduction step with buffered solution of anhydrous hydrazine to remove Mn-Fe oxide coatings. The "full cleaning" method includes another additional step to the "Cd cleaning" procedure, which requires treatment of the foraminiferal samples with alkaline diethylene-triamine-pentaacetic acid (DTPA) to remove barite. The reduction and DTPA steps are a standard procedure for Cd/Ca and Ba/Ca analyses, respectively [*Boyle and Keigwin*, 1985; *Lea and Boyle*, 1991; *Martin and Lea*, 2002], and because all elements can be analyzed simultaneously, it is tempting to apply the same cleaning procedure and measure all elements together. However, there is an ongoing debate whether the reduction step is necessary, if it is adequate or if it is even compromising the Mg/Ca analyses [*Pena et al*., 2005; *Martin and Lea*, 2002; *Rosenthal et al*., 2004; *Barker et al*., 2003; *Yu et al*., 2007b].

We applied two methods, the "Mg cleaning" [*Barker et al*., 2003] and the "full cleaning" [*Martin and Lea*, 2002], prior to the Mg/Ca analyses. We present first the differences in downcore *N. pachyderma* Mg/Ca owing to the use of the two different cleaning methods and, thereafter, we discuss the obtained results of variations in downcore Mg/Ca and $\delta^{18}O$ records in terms of paleoceanographic changes. We aim to constrain the evolution in the shallow subsurface hydrography in the southern Norwegian Sea during Heinrich stadials, the Last Glacial Maximum (LGM), and the last interglacial in connection with past regional climate change.

2. Methods

2.1. Minor/Trace Element Analyses in *N. pachyderma*

Only pristine specimens of *N. pachyderma* with no visible signs of dissolution were selected from size fraction 150–250 μm for minor/trace element analyses. For the first set of minor/trace element analyses, the foraminiferal tests (50–100 specimens) were gently crushed and cleaned following the "Mg cleaning" method [*Barker et al*., 2003] with a slight modification: the removal of coarse-grained silicate was omitted and instead the samples were centrifuged after dissolution (10 min, 6000 rpm) to separate any insoluble particles. The samples were analyzed using an ICP-OES (Agilent Technologies, 700 Series with autosampler (ASX-520 Cetac) and micro-nebulizer) at the Department of Geosciences, University of Bremen. Instrumental accuracy of the ICP-OES was monitored by analysis of an in-house standard solution with a Mg/Ca of 2.93 mmol/mol every five samples (long-term average of 2.917 mmol/mol, standard deviation (σ) = 0.04 mmol/mol, and relative standard deviation (RSD) = 1.4%). The average relative precision of Mg/Ca for 16 replicate samples that were cleaned and analyzed during different sessions is 9%. Seventeen samples (~6% of the entire analyzed samples) with high Al/Ca, Fe/Ca, Mn/Ca (>average + 2σ), and two samples with exceptionally high Mg/Ca values were not included in the interpretation of the record (Supporting Information Table S1). Eight samples with high Mn/Ca (>average + 2σ) from the interval 930–965 cm downcore (of mid-Eemian age) gave consistent Mg/Ca values with samples having relatively lower Mn/Ca from the same interval. These samples were thus included in the discussion.

For the second set of minor/trace element analyses performed on *N. pachyderma*, 60–160 pristine specimens were gently crushed, weighed, and cleaned following the "full cleaning" procedure of *Martin and Lea* [2002] with some slight modifications after *Pena et al*. [2005]. These modifications include the number of water rinses after the reduction and DTPA steps. The samples were also rinsed with NH_4OH [*Lea and Boyle*, 1991] after the treatment with the DTPA solution, instead of using 0.01N NaOH [*Martin and Lea*, 2002]. The

samples were then analyzed by iCAPQ Inductively Coupled Plasma Mass Spectrometry (ICP-MS) at Lamont Doherty Earth Observatory (LDEO) of Columbia University. Based on repeated measurements of in-house standard solutions, the intrarun precision is $<$1.4% and 1.9% for Mg/Ca and B/Ca, respectively. The analyses of five replicate samples, picked and cleaned separately, showed an average relative precision of 4.3 and 2.7% for Mg/Ca and B/Ca, respectively. All cleaning and dissolution steps for the second set of analyses were done in boron-free filtered laminar flow benches and using boron-free Milli-Q water. Four samples were omitted due to very high Al/Ca ($>$average $+ 2\sigma$) (Supporting Information Table S1). To evaluate potential instrumental bias between our ICP-MS and ICP-OES analyses, a suite of standards (ECRM 752-1, BAM RS3, and CMSI 1767) [*Greaves et al*., 2008] were measured by both laboratories. The interlaboratory accuracy for Mg/Ca is 2.6, 0.2, and 1.4% for ECRM 752-1, BAM RS3, and CMSI 1767, respectively. For both sets of analyses, blank samples were analyzed within every batch of samples in order to monitor potential contamination from reagents and vials.

Foraminiferal shell weights were determined on a Mettler XP6 microbalance before the analyses, and average shell weights were calculated using the number of tests in each sample. To calculate the weight loss during the cleaning procedure, the samples were also weighed after the cleaning.

2.2. Stable Oxygen Isotope Analyses

The δ^{18}O for the benthic foraminiferal species *Melonis barleeanus* for the upper 7 m and the planktic foraminiferal species *N. pachyderma* for the upper 8 m of the 11 m long core JM11-FI-19PC were published in *Ezat et al*. [2014] and *Hoff et al*. [2016], respectively. For the lower part of the core, $\sim$20 and 50 specimens of *M. barleeanus* (size fraction 150–315 μm) and *N. pachyderma* (size fraction 150–250 μm) were picked, respectively, for stable isotope analyses. The oxygen isotope analyses for both *N. pachyderma* and *M. barleeanus* were performed using a Finnigan MAT 251 mass spectrometer with an automated carbonate preparation device at MARUM, University of Bremen. The values are reported relative to the Vienna Pee Dee Belemnite (VPDB), calibrated by using National Bureau of Standards (NBS) reference materials 18, 19, and 20 and the external standard error is 0.07‰.

2.3. Age Model and Stratigraphy

The age model for JM11-FI-19PC core is based on well-dated tephra layers, magnetic susceptibility [*Ezat et al*., 2014], and planktic and benthic foraminiferal δ^{18}O values. Six tephra layers were counted and identified in the upper 7 m of JM11-FI-19PC [*Ezat et al*., 2014]. Five of these tephra layers (Saksunarvatn tephra, Vedde ash, Faroe Marine Ash Zone (FMAZ) II, FMAZ III, and North Atlantic Ash Zone (NAAZ) II) are well-known tephra from the study area and have been synchronized to their counterparts in the Greenland ice cores [*Wastegård et al*., 2006; *Davies et al*., 2008, 2010; *Griggs et al*., 2014]. In the lower part of the core, we visually identified four tephra layers (5e-Low/BAS-IV, 5e Midt/RHY, 5C-Midt/BAS, and 5a-top/BAS-I tephra layers) in the size fractions $>$100 and 63–100 μm. These four tephra layers were identified by the major and trace elemental composition of individual tephra shards in the nearby core LINK 16 [*Abbott et al*., 2014]. The correlation between the magnetic susceptibility of core JM-FI-19PC and core LINK 16 with location of the identified tephra layers confirms our visual identification (Supporting Information Figure S1).

Within the firm constraints of the identified tephra layers, the age model was subsequently refined by tying the start of DO interstadials as seen in the δ^{18}O records from the Greenland ice cores with the increases in magnetic susceptibility (Figure 2). The increase in magnetic susceptibility has been proposed to reflect increase in the strength of deep currents transporting the magnetic particles from the source (the Icelandic volcanic province) to the site of deposition [e.g., *Rasmussen et al*., 1996; *Kissel et al*., 1999]. In the original age model [*Ezat et al*., 2014], the boundary between HS1 and interstadial 1 was chosen at 190 cm core depth correlating with increase in magnetic susceptibility. This increase was very gradual from 198 to 190 cm core depth (Figure 2), while an abrupt and large increase in benthic foraminiferal δ^{18}O ($\sim$1‰) occurs at 197 cm core depth (Figure 2). Despite the different interpretations of the increase in benthic foraminiferal δ^{18}O [e.g., *Rasmussen and Thomsen et al*., 2004; *Meland et al*., 2008], there is a consensus that they mark the end of HS1 and the onset of deep convection similar to today [e.g., *Rasmussen and Thomsen*, 2004; *Meland et al*., 2008]. Thus, we adopted the 197 cm core depth as the start of interstadial 1. Eleven calibrated radiocarbon dates measured in *N. pachyderma* [*Ezat et al*., 2014] strongly support our tuned age model for the past 50 kyr (Supporting Information Figure S2).

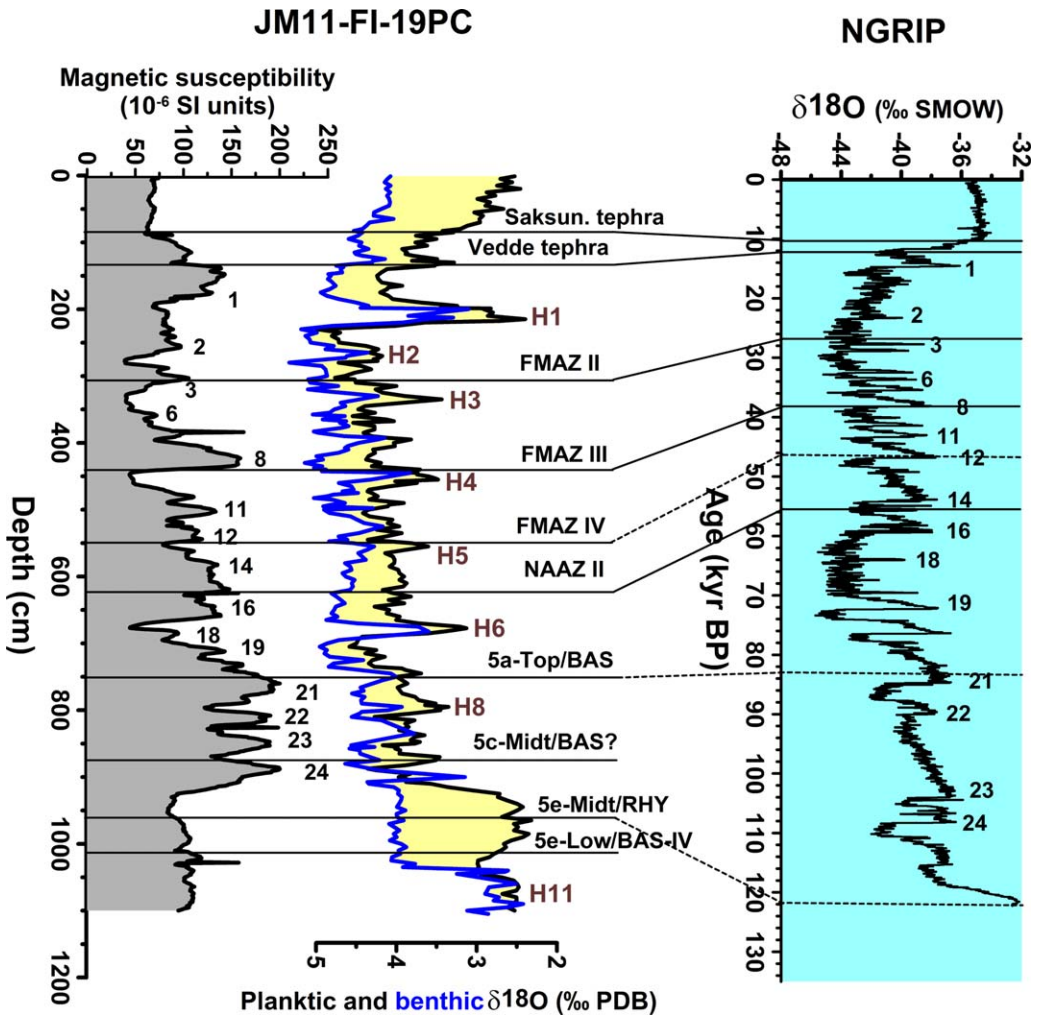

Figure 2. Correlation of magnetic susceptibility as well as planktic and benthic δ^{18}O in JM-FI-19PC [*Ezat et al*., 2014; *Hoff et al*., 2016, this study] and δ^{18}O values from Greenland Ice Core Project (NGRIP) on the Greenland Ice Core Chronology 2005 (GICC05) [*Seierstad et al*., 2014; *Rasmussen et al*., 2014, and references therein]. Solid black horizontal lines mark tephra layers identified in both marine and ice cores [*Davies et al*., 2008, 2010]. Tephra layers not yet confirmed in the ice cores and their potential location in ice records are shown by dashed black lines. Interstadial numbers (black) and Heinrich events (brown) are indicated.

The last interglacial "Eemian" (Marine Isotope Stage (MIS) 5e) can be recognized by a clearly developed gradient in the benthic and planktic foraminiferal δ^{18}O values. This gradient is similar to the gradient of the Holocene section (Figure 2). The lowermost part of JM11-FI-19PC with low planktic and benthic foraminiferal δ^{18}O values corresponds to HS11 in Termination II. We used the sharp increase in the benthic δ^{18}O values at 1035 cm core depth as an indication for the beginning of MIS 5e (Figure 2) and adopted an average sedimentation rate from the last deglaciation for HS11. The final age model is based on a radiocarbon date from a core-top sample (at 15 cm), 7 tephra layers, 21 magnetic susceptibility tie points, and 2 benthic δ^{18}O tie points.

2.4. Planktic Foraminiferal Assemblages

Core depth 50–255 cm spans the LGM to the mid Holocene (21–6 ka). From this interval at least 300 planktic foraminiferal specimens from the size fraction $>$100 μm were counted and identified to species level at 5 cm intervals (1 cm thick samples). *Kandiano and Bauch* [2002] pointed out that in cold polar areas more reliable temperature estimates can be obtained by using counts from planktic foraminiferal assemblages with mesh sizes $<$125 μm. Larger mesh-sizes tend to lose important small-sized subpolar species *Turborotalita quinqueloba* and *Globigerinita uvula*.

2.5. Estimation of *N. pachyderma* Calcification Temperatures

Neogloboquadrina pachyderma is the dominant planktic foraminiferal species in the polar and subpolar areas [*Bé and Tolderlund*, 1971] and therefore most often used in high latitude paleoceanographic reconstructions. However, identifying the mean calcification depth in the water column of *N. pachyderma* remains a challenge. Several studies from the Nordic Seas show a wide, but region-specific range of calcification depth of *N. pachyderma*. For example, *Simstich et al*. [2003] suggested a calcification depth for *N. pachyderma* between 70 and 250 m off Norway, between 70 and 130 m in the region of the East Greenland Current, and between 20 and 50 m in the highly productive Arctic water domain of the central Nordic Seas. In the central Irminger Sea, a recent study suggested a shallow (∼50 m) calcification depth for *N. pachyderma* based on the seasonal similarity in $\delta^{18}O$ recorded by *N. pachyderma* and local sea surface temperature [*Jonkers et al*., 2010, 2013]. In general, the signal recorded by *N. pachyderma* therefore seems likely to reflect a thick section of the upper water column, which makes *N. pachyderma* a suitable tracer of shallow subsurface water masses [*Bauch et al*., 1997], but not ideal for reconstructions of environmental conditions at the sea surface.

Core-top and sediment trap studies show an exponential Mg/Ca sensitivity of ∼9–10% per 1°C in several planktic foraminiferal species based on calibration of the foraminiferal Mg/Ca to $\delta^{18}O_{foram}$-derived temperatures [*Elderfield and Ganssen*, 2000; *Anand et al*., 2003]. The absence of such a clear relationship between *N. pachyderma* Mg/Ca and $\delta^{18}O$-derived temperatures in core-top and sediment trap data [*Meland et al*., 2006; *Nyland et al*., 2006; *Jonkers et al*., 2013] suggests that other factors affect the incorporation of Mg in shells of the species like seawater carbonate chemistry and salinity, variable degrees of encrustation [*Kozdon et al*., 2009], and/or undetermined species-specific mechanisms of bio-mineralization. Consequently, Mg/Ca measured in *N. pachyderma* should be treated carefully and may not directly be interpreted in terms of calcification temperature [*Hendry et al*., 2009; *Jonkers et al*., 2013].

Culture studies show that Mg/Ca in planktic foraminifera decrease with increasing seawater pH and carbonate ion concentration, but the sensitivity is species-specific. pH-sensitivity ranges from ∼7 to 16% per 0.1 unit change in pH for *Orbulina universa* and *Globigerina bulloides*, respectively [e.g., *Russell et al*., 2004]. Importantly, it was noted that the effect of pH on foraminiferal Mg/Ca is insignificant above modern pH values [*Russell et al*., 2004]. However, based on sediment trap samples off the West Antarctic peninsula, *Hendry et al*. [2009] found an increase in Mg/Ca in *N. pachyderma* by ∼10% per 10 μmol kg^{-1} increase in carbonate ion concentration, in clear conflict with the culture experiments that were performed on other planktic species. The carbonate ion concentration data in *Hendry et al*. [2009] are mainly derived from B/Ca measured in *N. pachyderma* using a calibration based on measurements in *Globorotalia inflata* from *Yu et al*. [2007a]. Although B/Ca in planktic foraminifera is shown to covary with seawater carbonate chemistry [*Yu et al*., 2007a; *Allen et al*., 2012], a quantitative assessment is complicated [*Allen et al*., 2012]. Because the study of *Hendry et al*. [2009] was performed on the same foraminiferal species and under oceanographic conditions likely not very different from the glacial and deglacial situation at our site, we attempted to correct for carbonate ion concentration influence on Mg/Ca assuming a 10% increase in Mg/Ca per 10 μmol kg^{-1} increase in carbonate ion concentration. For this, we used our B/Ca to calculate the carbonate ion concentration using the calibration from *Yu et al*. [2007a] similar to *Hendry et al*. [2009]. Although a species-specific calibration for B/Ca in *N. pachyderma* is now available [*Yu et al*., 2013], we chose to use the *Yu et al*. [2007a] calibration to be consistent with *Hendry et al*. [2009].

A sensitivity of 4–8% in Mg/Ca per salinity unit was recorded in other planktic foraminiferal species (for details see *Hönisch et al*. [2013]), but no empirical attempts have been done to test the salinity influence on Mg/Ca in shells of *N. pachyderma*. In addition, an independent proxy for seawater salinity is lacking. Thus, we did not attempt to correct for a possible salinity effect on Mg/Ca.

We estimated the temperature and $\delta^{18}O_{SW}$ based on both original Mg/Ca data and the carbonate ion concentration-corrected Mg/Ca data as described above. The Mg/Ca were used to calculate the calcification temperatures based on a Mg/Ca-temperature calibration: Mg/Ca = preexponential constant * exp (0.1T) [*Elderfield and Ganssen*, 2000], where the preexponential constant is calibrated to our core-top samples yielding a value of 0.4 and T is the temperature. We then calculated $\delta^{18}O_{SW}$ by removing the temperature effect from *N. pachyderma* $\delta^{18}O$ using the equation from *Shackleton* [1974]. We used the global eustatic sea level record of *Grant et al*. [2012] to correct for the temporal changes in ice volume, assuming a 1‰ increase

in $\delta^{18}O$ due to 120 m sea level drop [*Adkins et al*., 2002]. To convert from the Pee Dee Belemnite (PDB) scale for carbonate $\delta^{18}O$ to Standard Mean Ocean Water (SMOW) scale for water $\delta^{18}O$, 0.2 was added [*Shackleton*, 1974]. We calculated the uncertainty (2σ) in temperature and $\delta^{18}O_{SW}$ reconstructions as the square root of the sum of the squared analytical and calibration uncertainties. The analytical precision of Mg/Ca based on replicate foraminiferal samples is ~0.03 mmol/mol (which translates to ~0.4°C), whereas the uncertainty introduced by the Mg/Ca-temperature calibration equation is ~0.6°C [*Elderfield and Ganssen*, 2000]. Accordingly, the combined error in temperature reconstructions is ±0.7°C. Based on the combined effect of temperature error on $\delta^{18}O_{SW}$ (which translates to ~0.2‰ $\delta^{18}O$) and the analytical precision of foraminiferal $\delta^{18}O$ based on replicate analyses of NBS 19 (0.07‰), the combined error in our $\delta^{18}O_{SW}$ reconstructions is ±0.22‰.

3. Results and Discussion

3.1. Downcore Mg/Ca From "Mg Cleaning" and "Full Cleaning" Methods

The Mg/Ca results from the "Mg cleaning" and "full cleaning" methods are compared in Figure 3, along with Al/Ca, Fe/Ca, and Mn/Ca as monitors for possible contamination by clay minerals and/or Mn-oxyhydroxides/carbonates [*Boyle*, 1981; *Barker et al*., 2003]. Holocene samples cleaned with either method gave indistinguishable Mg/Ca values, while significant and nonsystematic offsets are observed downcore (Figure 3E). In general, the glacial and Eemian samples that were cleaned by the "full cleaning" method yielded lower Mg/Ca by 10–50% than when the "Mg cleaning" was applied. This decrease in the Mg/Ca is consistent with a decrease in Mn/Ca (Figure 3). Most Mg/Ca studies apply only the "Mg cleaning" method because the reductive step to remove metal coatings causes partial test dissolution and studies including the reduction step yield Mg/Ca ratios 10–15% lower than the "Mg cleaning" method [*Rosenthal et al*., 2004; *Barker et al*., 2003; *Yu et al*., 2007b]. However, it is still not clear if the systematic offset in Mg/Ca between the two cleaning methods is due to efficient removal of contaminant phases or dissolution [*Barker et al*., 2005; *Pena et al*., 2005].

If the decrease in our downcore Mg/Ca was caused by dissolution as a side effect from the extra cleaning [e.g., *Barker et al*., 2003; *Yu et al*., 2007b], we may expect this decrease to predominate in samples where the weight loss% during the cleaning process is higher. However, we observe the opposite; samples with largest sample weight loss% during cleaning yield almost identical Mg/Ca values from both cleaning methods (e.g., Holocene and interstadial 8), while most of the significant differences in Mg/Ca values occur at intervals with smallest sample weight loss% during the cleaning process (e.g., LGM and HS4) (Figure 3). To directly assess the effect of additional steps in the "full cleaning" method relative to the "Mg cleaning" method, weight loss% should be compared between the two methods (i.e., the weight loss due to the extra cleaning steps). The difference in weight loss% between the "full cleaning" and "Mg cleaning" methods (Δ weight loss%), when available, varies oppositely to Δ Mg/Ca (Figure 3F). Thus, it seems unlikely that the ΔMg/Ca is caused by partial dissolution as a side effect from the extra cleaning, albeit that the weight loss may be partly caused by fragmentation rather than laboratory dissolution during the cleaning.

In addition, specimens of pristine *N. pachyderma* were picked from 13 samples selected from different intervals to be run again based on the "Mg cleaning" method. Regardless of their apparent noise in Fe/Ca and Al/Ca, their Mg/Ca and Mn/Ca show the same trends as before with consistent values (Figure 4). When the "full cleaning" method was applied to samples from the same depths, considerable decreases in Mg/Ca only occurred in samples with high Mn/Ca from the "Mg cleaning" method (Figure 4). This indicates that the Mg/Ca decrease, when the full cleaning method applied is likely due to a more efficient removal of Mn contaminants. Figure 5 shows the relationships between ΔMg/Ca, ΔMn/Ca, and ΔFe/Ca for all samples that have been cleaned by both methodologies, which confirm that most of the removed contaminants due to the extra cleaning steps in the full cleaning method are Mn-oxides. However, the relation between the ΔMg/Ca and ΔMn/Ca is not linear (Figure 5), which can be due to a variable amount of Mn-contaminant coatings precipitated at different periods or changing composition of these coatings. It also seems that Mn-coatings on Eemian samples contain much less Mg than coatings in glacial samples (Figure 5). Finally, the "full cleaning" method might have removed contaminating phases other than Mn-contaminants that might have been trapped by such coatings and were only exposed (and hence released), by the removal of the Mn-oxide coatings [*Barker et al*., 2005]. Note that all our Mn/Ca values from the full cleaning method are

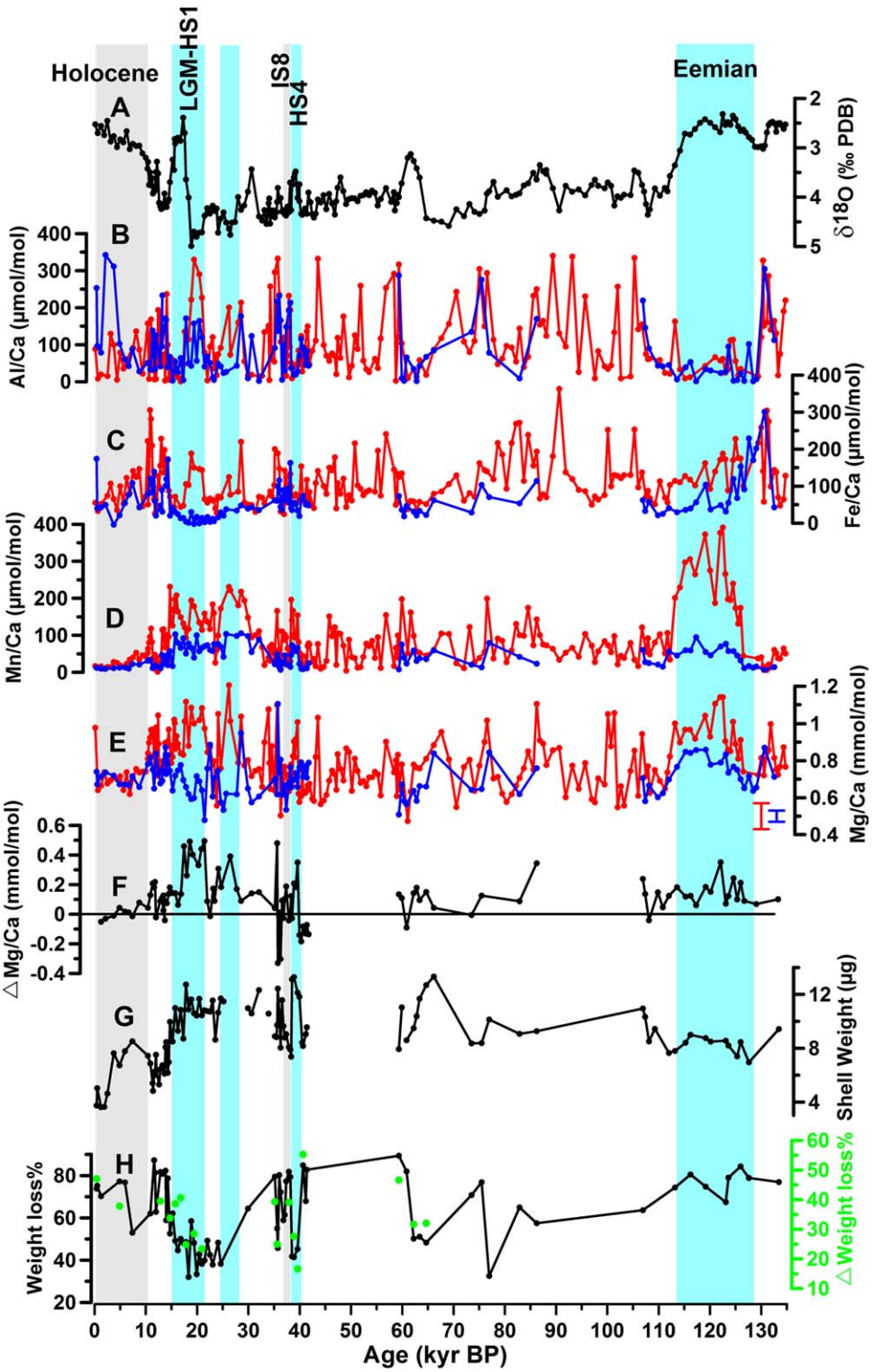

Figure 3. Comparison of downcore minor/trace element results for planktic foraminiferal species *Neogloboquadrina pachyderma* from the "Mg cleaning" (red) and "full cleaning" (blue) methods. (a) Oxygen isotopes measured in *N. pachyderma*. (b) Al/Ca in µmol/mol. (c) Fe/Ca in µmol/mol. (d) Mn/Ca in µmol/mol. (e) Mg/Ca in mmol/mol. Red and blue error bars close to the *y*-axis in Figure 3e represent the average relative precision of repeated foraminiferal samples for the "Mg cleaning" and "full cleaning" methods, respectively (see section 2). (f) Difference in Mg/Ca (ΔMg/Ca) between the two cleaning methods calculated by subtracting the Mg/Ca values from the "full cleaning" method from the Mg/Ca values from the "Mg cleaning" method (g) shell weight of *N. pachyderma* in µg. (h) Black line-scatter plot refers to weight loss% from samples cleaned by the full cleaning method, while green circles refer to weight loss% from the "full cleaning" minus the weight loss% from "Mg cleaning" methods (Δ weight loss%). Light blue bars refer to intervals with significant differences between the two cleaning methods and grey bars refer to intervals with almost no differences between the two cleaning methods. HS, Heinrich Stadial; LGM, Last Glacial Maximum; IS, Interstadial.

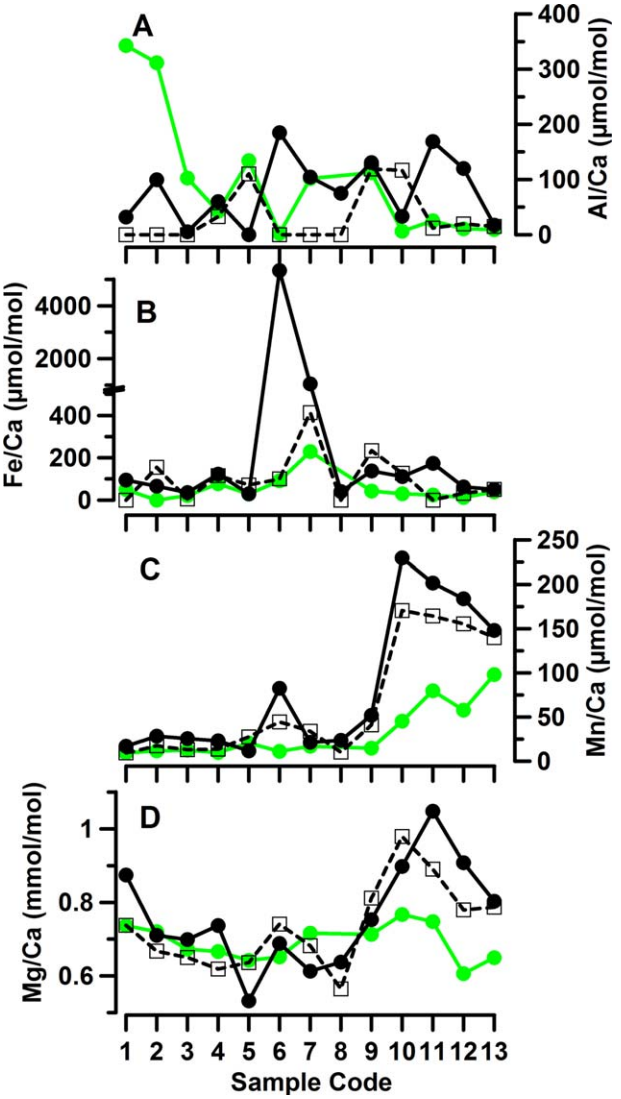

Figure 4. (a) Al/Ca, (b) Fe/Ca, (c) Mn/Ca, and (d) Mg/Ca for *N. pachyderma* cleaned by the "Mg cleaning" method (two runs, black circles and squares) and using the "full cleaning" method (one run, green circles) (see text for explanation). Note the break in the *y* axis of the Fe/Ca plot.

lower than 105 µmol/mol (Figure 3) indicating a minimal effect, if any, of diagenetic coatings on our results [*Boyle*, 1983; *Barker et al*., 2005]. Overall, this indicates that the "Mg cleaning" method was not sufficient to remove the different contaminant phases. We, therefore, limit our later discussion on the paleoceanography based on *N. pachyderma* Mg/Ca to the minor/trace element results from the "full cleaning" method although these results are of much lower resolution than the results from the "Mg cleaning" method.

3.2. Reconstruction of Conditions for the Last Glacial and Deglaciation

We estimated the calcification temperature and $\delta^{18}O_{SW}$ based on both original Mg/Ca data and the carbonate ion concentration-corrected Mg/Ca data using the B/Ca record and following *Hendry et al.* [2009] as described in section 2.5. During the late LGM (21–19 ka), the *N. pachyderma*-based temperature and $\delta^{18}O_{SW}$ are ~4.5°C and ~0.9‰, respectively. Using the corrected Mg/Ca data, the values are ~2.5°C and ~0.4‰ (Figure 6). Previous studies have shown conflicting temperature reconstructions for the LGM in the Nordic Seas. Planktic foraminiferal assemblage studies suggest the temperature during the LGM was ~4°C lower compared to modern values [e.g., *Pflaumann et al*., 2003], whereas alkenone data, dinocyst, and coccolith assemblage studies reveal temperatures up to 15°C (i.e., higher than modern temperatures) [e.g., *Rosell-Melé and Comes*, 1999; *de Vernal et al*., 2000; *Lévesque*, 1995]. It is still not clear if this discrepancy in temperature reconstructions reflects seasonal/depth gradients in the upper water column or taphonomic bias in some of these signal-carriers (see for review *de Vernal et al*. [2006]). Our temperature reconstructions suggest that the LGM temperatures at the calcification depth (and season) of *N. pachyderma* are ~1.5 or 3.5°C lower than Holocene temperatures based on the original or corrected Mg/Ca, respectively (Figure 7). We emphasize that the study of *Hendry et al*. [2009] is based on carbonate ion concentration data that are mainly derived from B/Ca measured in *N. pachyderma* using a calibration for *G. inflata* and not direct measurements. In addition, a quantification of the marine carbonate system using B/Ca in planktic foraminifera is complicated and other factors like salinity may have a significant effect on B/Ca [*Allen and Hönisch*, 2012; *Henehan et al*., 2015]. Furthermore, the suggested sensitivity of Mg/Ca to carbonate ion concentration in *Hendry et al*. [2009] is contrary to results from laboratory studies performed on other planktic foraminiferal species [e.g., *Russell et al*., 2004]. Future laboratory studies investigating the nontemperature factors that affect the Mg/Ca in *N. pachyderma* are therefore needed to better understand the glacial thermal structure of the upper water column in the Nordic Seas. Note that the main difference in temperature, when correcting the Mg/Ca for carbonate ion concentration following *Hendry et al*. [2009] is a decrease by ~2°C during the LGM, whereas it yields insignificant effects elsewhere in our record (Figure 6).

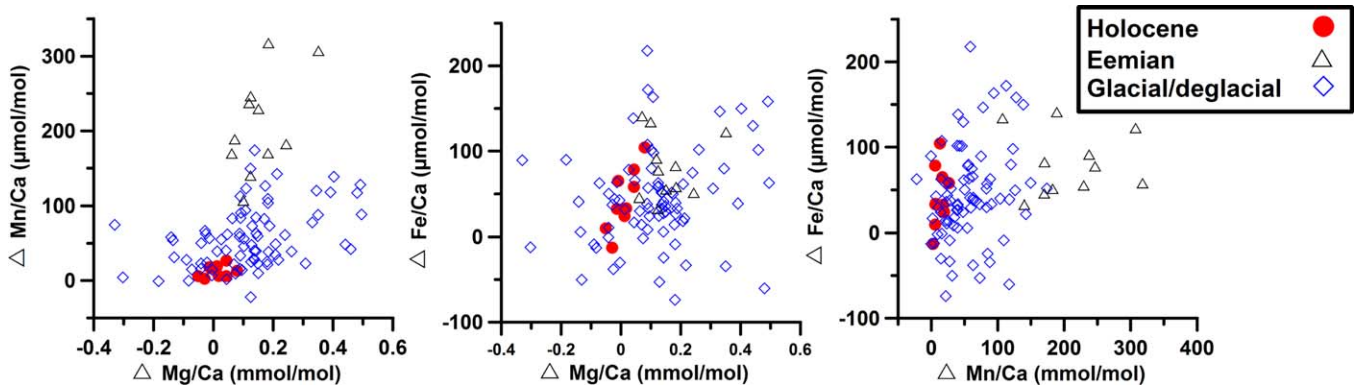

Figure 5. Relationship between the corresponding differences in Mg/Ca, Mn/Ca, and Fe/Ca for *N. pachyderma* from the "Mg cleaning" and "full cleaning" methods. ΔMg/Ca (ΔMn/Ca or ΔFe/Ca) is calculated by subtracting the Mg/Ca (Mn/Ca or Fe/Ca) from the "full cleaning" method from the Mg/Ca (Mn/Ca or Fe/Ca) from the "Mg cleaning" method.

During HS1, the temperature increased to ~6.5°C and the $\delta^{18}O_{SW}$ decreased to $-0.4‰$ (Figure 6). At the onset of the Bølling-Allerød (BA) interstadial (~14.6 ka), $\delta^{18}O_{SW}$ and temperature increased to $1‰$ and 7°C, respectively (Figure 6). The decrease in the $\delta^{18}O_{SW}$ values during HS1 precedes the increase in the calcification temperature (Figure 7). Addition of low $\delta^{18}O$ water from melt and meteoric water could have been responsible for the decrease in $\delta^{18}O_{SW}$ through a direct recording of the signal [e.g., *Bond et al*., 1993; *Fronval et al*., 1995; *Rasmussen et al*., 1996] or by transfer of the signal via brines deeper in the upper water column as in the Arctic Ocean today [*Hillaire-Marcel and de Vernal*, 2008], where *N. pachyderma* may have precipitated most of its calcite [e.g., *Kozdon et al*., 2009]. It is also notable that the increase in calcification temperature is not associated with a decrease in the % *N. pachyderma* (which decreases in relative abundance with decreasing influence of cold polar surface water). Thus, the increase in calcification temperature with no concomitant change in the % *N. pachyderma* (~80%) (Figure 7) can be explained by fresh water-induced stratification of the upper ocean and development of a halocline, at least during the calcification season of *N. pachyderma*. The evolution in % *N. pachyderma* and calcification temperature trends across HS1 from south of Iceland [*Thornalley et al*., 2010, 2011] are very similar to our site (Figure 7). This increase in the shallow subsurface water temperature may have eventually destabilized the water column at the end of HS1 and resulted in the erosion of the halocline and the resumption of the open ocean convection in the Nordic Seas [e.g., *Knorr and Lohman*, 2007].

Our Mg/Ca record based on the "full cleaning" method is of too low resolution to resolve all of the DO events. Yet our data show decreases in the $\delta^{18}O_{SW}$ values from the average glacial $\delta^{18}O_{SW}$ ($\sim 1‰$) to $\sim -0.4‰$ during HS6 and to $0.5‰$ during HS2, HS3, and HS4 (Figure 6). The calcification temperature increases during HS2, similar to HS1. The temperature evolution across HS6, HS4, and HS3 does not show a clear evidence of temperature change (Figure 6). Studies based on benthic foraminiferal assemblages and benthic geochemical signatures have suggested an increase in the temperature of the intermediate water (800–2000 m water depth) in the SE Nordic Seas for almost all stadials [e.g., *Rasmussen et al*., 1996; *Rasmussen and Thomsen*, 2004; *Ezat et al*., 2014]. At the shallow subsurface calcification depth of *N. pachyderma* a temperature increase apparently only occurs during some stadial events and not all. Modeling studies suggested that weakening in the Atlantic Meridional Overturning Circulation (AMOC) results in increased inflow of subsurface warm Atlantic water into the northern North Atlantic [e.g., *Knorr and Lohman*, 2007]. A recent study [*Böhm et al*., 2015] suggested that during the past 150 kyr, substantial suppression of the AMOC occurred only during Heinrich stadials close to the glacial maxima (i.e., HS1, HS2, and HS11). This agrees with our findings that these Heinrich stadial events close to the glacial maxima (HS1, HS2, and HS11, see the next section for HS11) are associated with significant thickening of the Atlantic water in the subsurface Nordic Seas.

3.3. Reconstructions of Termination II, Eemian, and Last Glacial Inception

During the latest part of Termination II (=HS11), both *N. pachyderma* and the benthic foraminiferal records show similar $\delta^{18}O$ values ($=2.7‰$) (Figure 8). At the beginning of the Eemian interglacial, the two records diverge significantly from each other. The $\delta^{18}O$ values of *N. pachyderma* increase slightly to $3‰$, while the

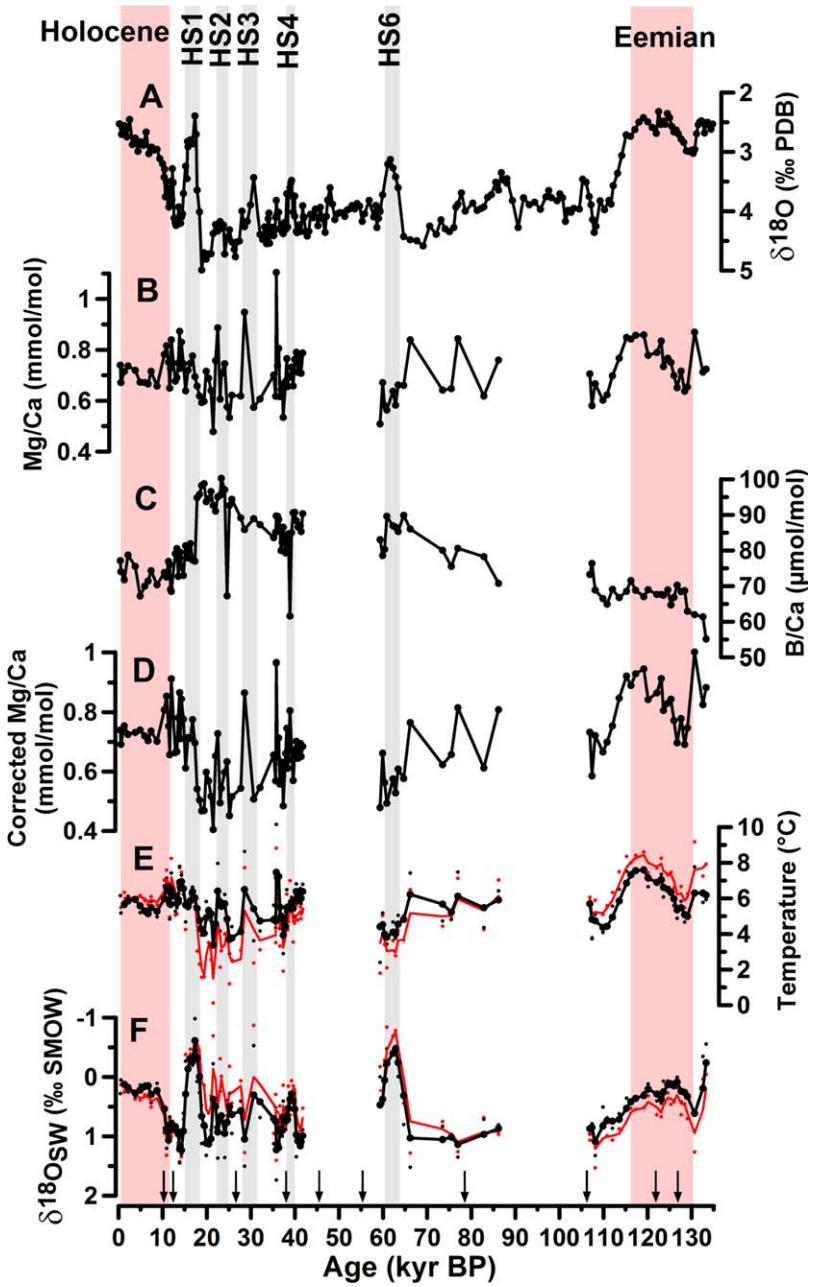

Figure 6. Downcore reconstructions of temperature and seawater $\delta^{18}O$ at calcification depth and season of *N. pachyderma*. (a) $\delta^{18}O_{calcite}$. (b) Mg/Ca in mmol/mol. (c) B/Ca in µmol/mol. (d) Corrected Mg/Ca based on B/Ca (see section 2.5 for explanation). (e) Temperature based on raw Mg/Ca data (black circles) and Mg/Ca values corrected for carbonate ion concentration Mg/Ca (red circles). Black and red lines represent 3-point moving averages based on raw Mg/Ca and corrected Mg/Ca, respectively. (f) Seawater $\delta^{18}O$, calculated using raw Mg/Ca-based temperatures (black circles) and using corrected Mg/Ca-based temperatures (red circles). Solid lines represent 3-point moving averages. Arrows above the *x* axis refer to the location of the tephra layers (see Figure 2). HS, Heinrich Stadial.

benthic $\delta^{18}O$ values increase abruptly to 4‰ (Figure 8). This is similar to previous studies from the southern Norwegian Sea [*Balbon*, 2000; *Rasmussen et al*., 2003a] as well as in the central and northern parts of the Norwegian Sea [*Fronval et al*., 1998]. At the same time the calcification temperature of *N. pachyderma* decreased by ~1.5°C. The high deposition of IRD in the area [*Rasmussen et al*., 2003a] and the low $\delta^{18}O_{SW}$ during late HS11 (Figure 8) indicate the presence of icebergs and melt water at the surface (see section 3.2 for discussing the low $\delta^{18}O_{SW}$ recorded by *N. pachyderma*). Thus, the relatively high temperatures based on Mg/Ca in *N. pachyderma* (~6.5°C) most likely indicate the presence of a strong halocline similar to HS1.

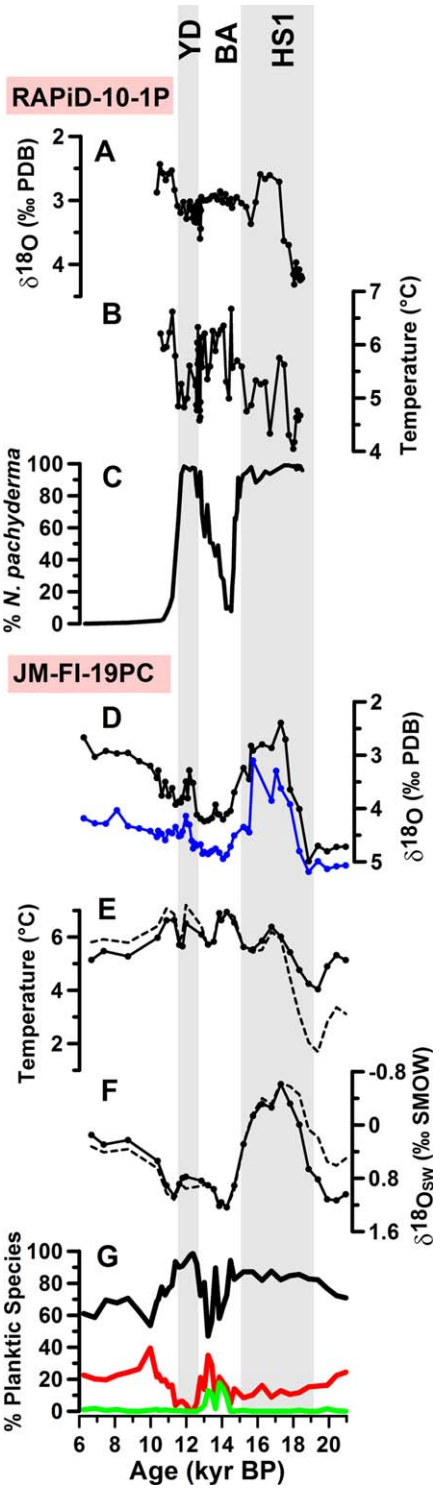

Figure 7. Shallow subsurface hydrographic details of the last deglaciation from (a–c) south of Iceland [*Thornalley et al*., 2010, 2011] and (d–g) southern Norwegian Sea [*Ezat et al*., 2014; *Hoff et al*., 2016, this study]. (a) δ^{18}O values measured on *N. pachyderma*. (b) Temperature based on Mg/Ca measured on *N. pachyderma*. (c) % *N. pachyderma*. (d) δ^{18}O values measured on *N. pachyderma* (black) and *Melonis barleeanus* (blue). (e) Temperature based on Mg/Ca measured on *N. pachyderma*. (f) Seawater δ^{18}O based on Mg/Ca and δ^{18}O values measured on *N. pachyderma*. Solid and dashed lines in Figures 7e and 7f are 3-point moving averages based on raw and corrected Mg/Ca, respectively. (g) Percentages of planktic foraminiferal species: % *N. pachyderma* in black, % *Turborotalia quinqueloba* in red, and % *Globigerinita uvula* in green. HS, Heinrich Stadial; BA, Bølling-Allerød interstadials; YD, Younger Dryas. The original age model for sediment core RAPiD-10-1P in [*Thornalley et al*., 2010] is slightly modified by aligning it to JM-FI-19PC using the start of the deglacial decrease in δ^{18}O in *N. pachyderma* as a tuning marker.

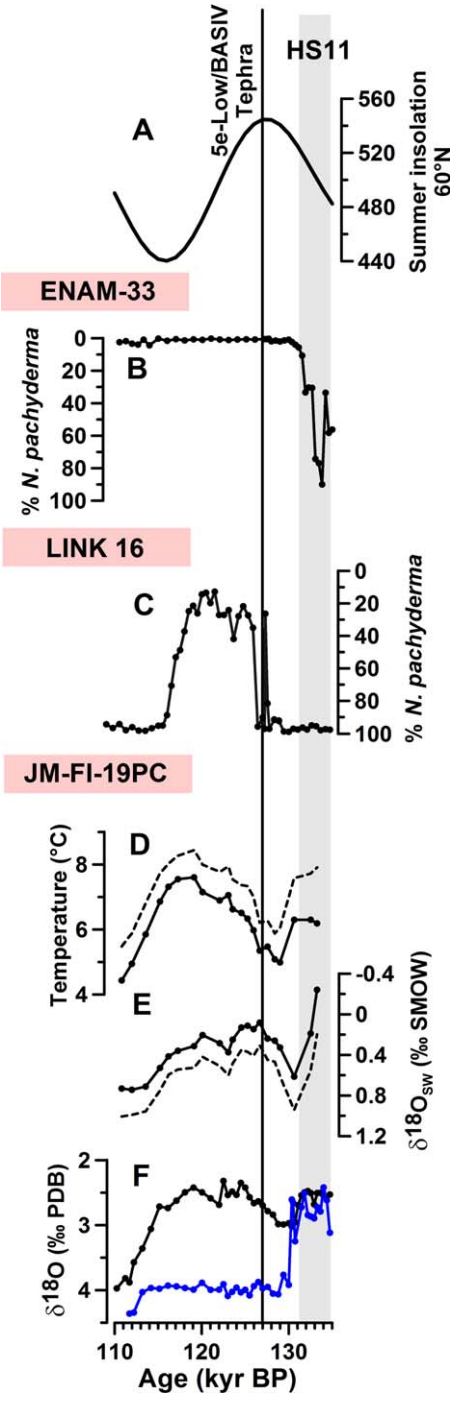

Figure 8. Climate records for the last interglacial. (a) Summer solar insolation at 60°N [*Berger*, 1978]. (b) % *N. pachyderma* from sediment core ENAM-33 [*Rasmussen et al.*, 2003a]. (c) % *N. pachyderma* from sediment core LINK 16 [*Abbott et al.*, 2014]. (d) Temperature based on Mg/Ca measured on *N. pachyderma*. (e) Seawater $\delta^{18}O$ based on Mg/Ca and $\delta^{18}O$ values measured on *N. pachyderma*. Solid and dashed lines in Figures 8d and 8e are 3-point moving averages based on raw and corrected Mg/Ca respectively. (f) Foraminiferal $\delta^{18}O$ values measured in *M. barleeanus* (blue) and *N. pachyderma* (black). HS, Heinrich Stadial.

The evolution in shallow subsurface temperature during the Eemian based on our Mg/Ca measured in *N. pachyderma* is in good agreement with previous estimates based on planktic foraminiferal assemblages and dinoflagellate cysts [*Rasmussen et al.*, 2003a; *Van Nieuwenhove et al.*, 2011; *Abbott et al.*, 2014] documenting a delay in the Eemian peak warmth compared to the North Atlantic, and a late Eemian warming in the southeastern Nordic Seas [see also *Capron et al.*, 2014]. The *N. pachyderma*-based shallow subsurface temperature gradually increased from 5°C during the early Eemian (130–126 ka) reaching its maximum ~8°C during the late Eemian and early part of the glacial inception (120–116 ka) (Figure 8), which is ~2°C higher than during the Holocene (Figure 6).

Although the IRD content decreased significantly at the onset of the Eemian (~130 ka), there is almost no change in the % of *N. pachyderma* (>85%) from HS11 into the early Eemian until ~126 ka indicating continued presence of polar/Arctic water at the surface [*Fronval and Jansen*, 1997; *Fronval et al.*, 1998; *Rasmussen et al.*, 2003a]. The $\delta^{18}O_{SW}$ at the calcification depth and season of *N. pachyderma* (=~0.6‰) was ~0.25‰ higher during the early Eemian (130–126 ka) than the average values for the mid/late Eemian and the Holocene (Figure 8). Assuming that the $\delta^{18}O_{SW}$ composition of the freshwater sources and their relative contribution in our area did not change significantly through the Eemian and the Holocene, the high $\delta^{18}O_{SW}$ suggests the presence of a high-salinity water mass. This may indicate the presence of near-surface Atlantic water below a thin layer of polar/Arctic water, as the polar/Arctic water signature is not recorded by the shallow subsurface-dwelling *N. pachyderma*. Such shallow subsurface inflow of Atlantic water is necessary to maintain deep outflow from this area into the North Atlantic as previously suggested due to the dominance of modern-like benthic foraminifera [*Rasmussen et al.*, 1999; *Rasmussen et al.*, 2003a]. This suggests that despite the relatively cold conditions (compared to average interglacial temperatures) and southward advance of the Arctic front during the early Eemian, the overturning circulation in the Nordic Seas was active, although it was probably weaker/shallower compared to modern.

The late Eemian warming in the eastern Nordic seas, which extended to the time of summer insolation minimum at 60°N (Figure 8) has been explained by weakening of the subpolar gyre [e.g., *Born et al.*, 2011]. Records show cooling at that time in the western Iceland Sea, which gives further evidence for the hypothesis of weakening of the subpolar gyre [*Van Nieuwenhove et al.*, 2013]. The temperature gradually decreased after 115 ka to ~5°C at the inception (at 111 ka) of the Weichselian glacial (Figure 8). The increase in the *N. pachyderma*-based $\delta^{18}O_{SW}$ during the glacial inception (Figure 8) may be due

to an increase in the local salinity and/or in the source water salinity. This suggests persistent Atlantic water inflow during the glacial inception, which as previously suggested may have played an important role in the early growth of northern ice sheets through the amplification of sea to land moisture fluxes [e.g., *Ruddiman et al*., 1980; *Risebrobakken et al*., 2007].

4. Conclusions

We combined measurements of Mg/Ca and $\delta^{18}O$ in shells of the planktic foraminiferal species *N. pachyderma* to reconstruct the shallow subsurface hydrography during the last interglacial-glacial cycle. First, we reported the downcore Mg/Ca, Al/Ca, Mn/Ca, Fe/Ca results from two different cleaning methods ("Mg cleaning" and "full cleaning"), along with weight loss% during the cleaning. We showed that the "Mg cleaning" method was not sufficiently effective in removing different contaminants. This may also apply to areas with similar diagenetic history and thus we recommend, similar to previous studies [*Barker et al*., 2005], that a screening downcore test for different cleaning protocols should be applied before deciding which cleaning protocol to use.

Low seawater $\delta^{18}O$, relatively high temperature and dominance of *N. pachyderma* (>80%) are recorded during Heinrich Stadial (HS)1, which suggests a strong stratification in the upper water column and likely a shallow subsurface inflow of Atlantic water below a well-developed halocline. Similar hydrographic features were also observed during HS11 in Termination II. Our Mg/Ca record based on the full cleaning method is discontinuous and in certain intervals of low resolution and was not capable of resolving all glacial millennial scale climatic events. However, low $\delta^{18}O_{SW}$ values were also recorded for HS2, HS3, HS4, and HS6.

The evolution in the Mg/Ca-based shallow subsurface temperatures during the Eemian generally agrees with previous estimates based on planktic foraminiferal assemblages and dinoflagellate cysts documenting the delay of the last interglacial "Eemian" warm peak in the eastern Nordic Seas relative to the North Atlantic. However, our high values of $\delta^{18}O_{SW}$ during the early Eemian may indicate a shallow subsurface inflow of Atlantic water below a thin layer of polar/Arctic water.

Acknowledgments
We sincerely thank B. Hönisch for helpful discussions and comments on earlier versions of the manuscript and two anonymous reviewers for constructive comments and suggestions. J. Ruprecht is thanked for great support in the laboratory, K. Esswein and P. DeMenocal for running the ICP-MS at LDEO. Also thanks to U. Hoff, L. Pena, T. Dahl, M. Segl, S. Pape, J. Farmer, K. Allen, E. Ellingsen, I. Hald, K. Monsen, N. L. Rasmussen, and Y. Sen for technical support. This research was funded by UiT, Arctic University of Norway, the Mohn Foundation and supported by the Research Council of Norway through its Centres of Excellence funding scheme, project 223259. The data used are listed in the Supporting Information.

References

Abbott, P. M., W. E. N. Austin, S. M. Davies, N. J. G. Pearce, T. L. Rasmussen, S. Wastegård, and J. Brendryen (2014), Re-evaluation and extension of the Marine Isotope Stage 5 tephrostratigraphy of the Faroe Islands region: The cryptotephra record, *Palaeogeogr. Palaeoclim. Palaeoecol.*, *409*, 153–168, doi:10.1016/j.palaeo.2014.05.004.

Adkins, J. F., K. McIntyre, and D. P. Schrag (2002), The salinity, temperature, and $\delta^{18}O$ of the Glacial Deep Ocean, *Science*, *298*, 1769–1773, doi:10.1126/science.1076252.

Allen, K. A., and B. Hönisch (2012), The planktic foraminiferal B/Ca proxy for seawater carbonate chemistry: A critical evaluation, *Earth Planet. Sci. Lett.*, *345–348*, 203–211, doi:10.1016/j.epsl.2012.06.012.

Anand, P., H. Elderfield, and M. H. Conte (2003), Calibration of Mg/Ca thermometry in planktonic foraminifera from a sediment trap time series, *Paleoceanography*, *18*(2), 1050, doi:10.1029/2002PA000846.

Bahr, A., J. Schönfeld, J. Hoffmann, S. Voigt, R. Aurahs, M. Kucera, S. Flögel, A. Jentzen, and A. Gerdes (2013), Comparison of Ba/Ca and as freshwater proxies: A multi-species core-top study on planktonic foraminifera from the vicinity of the Orinoco River mouth, *Earth Planet. Sci. Lett.*, *383*, 45–57, doi:10.1016/j.epsl.2013.09.036.

Balbon, E. (2000), Variabilite climatique et circulation thermohaline dans l'Ocean Atlantique nord eten Mer de Norvège au cours du Quaternaire Superieur, PhD dissertation, Univ. of Paris, Paris.

Barker, S., M. Greaves, and H. Elderfield (2003), A study of cleaning procedures used for foraminiferal Mg/Ca paleothermometry, *Geochem. Geophys. Geosyst.*, *4*(9) 8407, doi:10.1029/2003GC000559.

Barker, S., I. Cacho, H. Benway, and K. Tachikawa (2005), Planktonic foraminiferal Mg/Ca as a proxy for past oceanic temperatures: A methodological overview and data compilation for the Last Glacial Maximum, *Quat. Sci. Rev.*, *24*, 821–834, doi:10.1016/j.quascirev.2004.07.016.

Barker, S., P. Diz, M. J. Vautravers, J. Pike, G. Knorr, I. R. Hall, and W. S. Broecker (2009), Interhemispheric Atlantic seesaw response during the last deglaciation. *Nature*, *457*, 1097–1102.

Barker, S., G. Knorr, R. L. Edwards, F. Parrenin, A. E. Putnam, L. C. Skinner, E. Wolff, and M. Ziegler (2011), 800,000 years of abrupt climate variability, *Science*, *334*, 347–351, doi:10.1126/science.1203580.

Bauch, D., J. Carstens, and G. Wefer (1997), Oxygen isotope composition of living *Neogloboquadrina pachyderma* (sin.) in the Arctic Ocean, *Earth Planet. Sci. Lett.*, *146*, 47–58, doi:10.1016/S0012-821X(96)00211-7.

Bauch, H. A., H. Erlenkeuser, R. F. Spielhagen, U. Struck, J. Matthiessen, J. Thiede, and J. Heinemeier (2001), A multiproxy reconstruction of the evolution of deep and surface waters in the subarctic Nordic seas over the last 30,000 years, *Quat. Sci. Rev.*, *20*, 659–678.

Bé, A. W. H., and D. S. Tolderlund (1971), Distribution and ecology of living planktonic foraminifera in surface waters of the Atlantic and Indian Oceans, in *The Micropaleontology of the Oceans*, edited by B. M. Funnel and W. R. Riedel, pp. 105–149, Cambridge Univ. Press, London, U. K.

Berger, A. (1978), Long-term variations of caloric insolation resulting from the earth's orbital elements, *Quat. Res.*, *9*, 139–167, doi:10.1016/0033-5894(78)90064-9.

Böhm, E., J. Lippold, M. Gutjahr, M. Frank, P. Blaser, B. Antz, J. Fohlmeister, N. Frank, M. B. Andersen, and M. Deininger (2015), Strong and deep Atlantic meridional overturning circulation during the last glacial cycle, *Nature*, *517*(7532), 73–76, doi:10.1038/nature14059.

Bond, G., W. Broecker, S. Johnsen, J. McManus, L. Labeyrie, J. Jouzel, and G. Bonani (1993), Correlations between climate records from North Atlantic sediments and Greenland ice, *Nature*, *365*, 143–147.

Born, A., K. H. Nisancioglu, and B. Risebrobakken (2011), Late Eemian warming in the Nordic Seas as seen in proxy data and climate models, *Paleoceanography*, *26*, PA2207, doi:10.1029/2010PA002027.

Boyle, E. A. (1981), Cadmium, zinc, copper, and barium in foraminifera tests, *Earth Planet. Sci. Lett.*, *53*(1), 11–35, doi:10.1016/0012-821X(81)90022-4.

Boyle, E. A. (1983), Manganese carbonate overgrowths on foraminifera tests, *Geochim. Cosmochim. Acta*, *47*, 1815–1819.

Boyle, E. A., and L. D. Keigwin (1985), Comparison of Atlantic and Pacific paleochemical records for the last 215,000 years: Changes in deep ocean circulation and chemical inventories, *Earth Planet. Sci. Lett.*, *76*, 135–150, doi:10.1016/0012-821X(85)90154-2.

Broecker, W. S. (1994), Massive iceberg discharges as triggers for global climate change, *Nature*, *372*, 421–424.

CAPE-Last Interglacial Project Members (2006), Last Interglacial Arctic warmth confirms polar amplification of climate change, *Quat. Sci. Rev.*, *25*, 1383–1400.

Capron, E., A. Govin, E. J. Stone, V. Masson-Delmotte, S. Mulitza, B. Otto-Bliesner, T. L. Rasmussen, L. C. Sime, C. Waelbroeck, and E. W. Wolff (2014), Temporal and spatial structure of multi-millennial temperature changes at high latitudes during the Last Interglacial, *Quat. Sci. Rev.*, *103*, 116–133, doi:10.1016/j.quascirev.2014.08.018.

Craig, H. (1961), Isotopic variations in meteoric waters, *Science*, *133*, 1702–1703, doi:10.1126/science.133.3465.1702.

Dansgaard, W. (1964), Stable isotopes in precipitation, *Tellus*, *16*, 436–468, doi:10.1111/j.2153-3490.1964.tb00181.x.

Dansgaard, W., et al. (1993), Evidence for general instability of past climate from a 250-kyr ice-core record, *Nature*, *364*, 218–220.

Davies, S. M., S. Wastegård, T. L. Rasmussen, A. Svensson, S. J. Johnsen, J. P. Steffensen, and K. K. Andersen (2008), Identification of the Fugloyarbanki tephra in the NGRIP ice core: A key tie-point for marine and ice-core sequences during the last glacial period, *J. Quat. Sci.*, *23*, 409–414, doi:10.1002/jqs.1182.

Davies, S. M., S. Wastegård, P. M. Abbott, C. Barbante, M. Bigler, S. J. Johnsen, T. L. Rasmussen, J. P. Steffensen, A. Svensson (2010), Tracing volcanic events in the NGRIP ice-core and synchronising North Atlantic marine records during the last glacial period, *Earth Planet. Sci. Lett.*, *294*, 69–79, doi:10.1016/j.epsl.2010.03.004.

Dekens, P. S., D. W. Lea, D. K. Pak, and H. J. Spero (2002), Core top calibration of Mg/Ca in tropical foraminifera: Refining paleotemperature estimation, *Geochem. Geophys. Geosyst.*, *3*, 1–29, doi:10.1029/2001GC000200.

de Vernal, A., C. Hillaire-Marcel, J.-L., Turon, and J. Matthiessen (2000), Reconstruction of sea-surface temperature, salinity, and sea-ice cover in the northern North Atlantic during the last glacial maximum based on dinocyst assemblages, *Can. J. Earth Sci.*, *37*, 725–750.

de Vernal, A., A. Rosell-Melé, M. Kucera, C. Hillaire-Marcel, F. Eynaud, M. Weinelt, T. Dokken, and M. Kageyama (2006), Comparing proxies for the reconstruction of LGM sea-surface conditions in the northern North Atlantic, *Quat. Sci. Rev.*, *25*, 2820–2834, doi:10.1016/j.quascirev.2006.06.006.

Drijfhout, S., S. Bathiany, C. Beaulieu, V. Brovkin, M. Claussen, C. Huntingford, M. Scheffer, G. Sgubin, and D. Swingedouw (2015), Catalogue of abrupt shifts in Intergovernmental Panel on Climate Change climate models, *Proc. Natl. Acad. Sci. U. S. A.*, *112*, E5777–E5786.

Elderfield, H., and G. Ganssen (2000), Past temperature and δ^{18}O of surface ocean waters inferred from foraminiferal Mg/Ca ratios, *Nature*, *405*, 442–445.

Eldevik, T., J. E. Ø. Nilsen, D. Iovino, K. A. Olsson, A. B. Sandø, and H. Drange (2009), Observed sources and variability of Nordic seas overflow, *Nat. Geosci.*, *2*, 406–410.

Emiliani, C. (1955), Pleistocene temperatures, *J. Geol.*, *63*, 538–578, doi:10.2307/30080906.

Ezat, M. M., T. L. Rasmussen, and J. Groeneveld (2014), Persistent intermediate water warming during cold stadials in the southeastern Nordic seas during the past 65 k.y., *Geology*, *42*, 663–666, doi:10.1130/g35579.1.

Friedrich, T., and A. Timmermann (2012), Millennial-scale glacial meltwater pulses and their effect on the spatiotemporal benthic δ^{18}O variability, *Paleoceanography*, *27*, PA3215, doi:10.1029/2012PA002330.

Fronval, T., and E. Jansen (1997), Eemian and Early Weichselian (140–60 ka) paleoceanography and paleoclimate in the Nordic Seas with comparisons to Holocene conditions, *Paleoceanography*, *12*, 443–462, doi:10.1029/97PA00322.

Fronval, T., E. Jansen, J. Bloemendal, and S. Johnsen (1995), Oceanic evidence for coherent fluctuations in Fennoscandian and Laurentide ice sheets on millennium timescales, *Nature*, *374*, 443–446.

Fronval, T., E. Jansen, H. Haflidason, and H. P. Sejrup (1998), Variability in surface and deep water conditions in the Nordic seas during the last interglacial period, *Quat. Sci. Rev.*, *17*, 963–985, doi:10.1016/S0277-3791(98)00038-9.

Galaasen, E. V., U. S. Ninnemann, N. Irvali, H. F. Kleiven, Y. Rosenthal, C. Kissel, and D. A. Hodell (2014), Rapid reductions in North Atlantic deep water during the peak of the last interglacial period, *Science*, *343*, 1129–1132.

Grant, K. M., E. J. Rohling, M. Bar-Matthews, A. Ayalon, M. Medina-Elizalde, C. Bronk Ramsey, C. Satow, and A. P. Roberts (2012), Rapid coupling between ice volume and polar temperature over the past 150,000 years, *Nature*, *491*, 744–747.

Greaves, M., et al. (2008), Interlaboratory comparison study of calibration standards for foraminiferal Mg/Ca thermometry, *Geochem. Geophys. Geosyst.*, *9*, Q08010, doi:10.1029/2008GC001974.

Griggs, A. J., S. M. Davies, P. M. Abbott, T. L. Rasmussen, and A. P. Palmer (2014), Optimising the use of marine tephrochronology in the North Atlantic: A detailed investigation of the Faroe Marine Ash Zones II, III, and IV, *Quat. Sci. Rev.*, *106*, 122–139.

Hansen, B., and S. Østerhus (2000), North Atlantic–Nordic Seas exchanges, *Prog. Oceanogr.*, *45*, 109–208, doi:10.1016/S0079-6611(99)00052-X.

Heinrich, H. (1988), Origin and consequences of cyclic ice rafting in the Northeast Atlantic Ocean during the past 130,000 years, *Quat. Res.*, *29*, 142–152, doi:10.1016/0033-5894(88)90057-9.

Hemming, S. R. (2004), Heinrich events: Massive late Pleistocene detritus layers of the North Atlantic and their global climate imprint, *Rev. Geophys.*, *42*, RG1005, doi:10.1029/2003RG000128.

Hendry, K. R., R. E. M. Rickaby, M. P. Meredith, and H. Elderfield (2009), Controls on stable isotope and trace metal uptake in *Neogloboquadrina pachyderma* (sinistral) from an Antarctic sea-ice environment, *Earth Planet. Sci. Lett.*, *278*, 67–77, doi:10.1016/j.epsl.2008.11.026.

Henehan, M. J., M. J., G. L. Foster, J. W. B. Rae, K. C. Prentice, J. Erez, H. C. Bostock, B. J. Marshall, and P. A. Wilson (2015), Evaluating the utility of B/Ca ratios in planktic foraminifera as a proxy for the carbonate system: A case study of *Globigerinoides ruber*, *Geochem. Geophys. Geosyst.*, *16*, 1052–1069, doi:10.1002/2014GC005514.

Hillaire-Marcel, C., and A. de Vernal (2008), Stable isotope clue to episodic sea ice formation in the glacial North Atlantic, *Earth Planet. Sci. Lett.*, *268*, 143–150, doi:10.1016/j.epsl.2008.01.012.

Hoff, U., T. L. Rasmussen, R. Stein, M. M. Ezat, and K. Fahl (2016), Sea ice and millennial-scale climate variability in the Nordic seas 90 ka to present, *Nat. Commun.*, *7*, 12247, doi:10.1038/ncomms12247.

Hönisch, B., K. A. Allen, A. D. Russell, S. M. Eggins, J. Bijma, H. J. Spero, D. W. Lea, and J. Yu (2011), Planktic foraminifers as recorders of seawater Ba/Ca, *Mar. Micropaleontol.*, *79*, 52–57, doi:10.1016/j.marmicro.2011.01.003.

Hönisch, B., K. A. Allen, D. W. Lea, H. J. Spero, S. M. Eggins, J. Arbuszewski, P. B. deMenocal, Y. Rosenthal, A. D. Russell, and H. Elderfield (2013), The influence of salinity on Mg/Ca in planktic foraminifers—Evidence from cultures, core-top sediments and complementary $\delta^{18}O$, *Geochim. Cosmochim. Acta*, *121*, 196–213, doi:10.1016/j.gca.2013.07.028.

Irvali, N., U. S. Ninnemann, E. V. Galaasen, Y. Rosenthal, D. Kroon, D. W. Oppo, H. F. Kleiven, K. F. Darling, and C. Kissel (2012), Rapid switches in subpolar North Atlantic hydrography and climate during the Last Interglacial (MIS 5e), *Paleoceanography*, *27*, PA2207, doi:10.1029/2011PA002244.

Jakobsen, P. K., M. H. Ribergaard, D. Quadfasel, T. Schmith, and C. W. Hughes (2003), Near-surface circulation in the northern North Atlantic as inferred from Lagrangian drifters: Variability from the mesoscale to interannual, *J. Geophys. Res.*, *108*(C8), 3251, doi:10.1029/2002JC001554.

Jonkers, L., G.-J. A. Brummer, F. J. C. Peeters, H. M. van Aken, and M. F. De Jong (2010), Seasonal stratification, shell flux, and oxygen isotope dynamics of left-coiling *N. pachyderma* and *T. quinqueloba* in the western subpolar North Atlantic, *Paleoceanography*, *25*, PA2204, doi:10.1002/palo.20018.

Jonkers, L., P. Jiménez-Amat, P. G. Mortyn, and G.-J. A. Brummer (2013), Seasonal Mg/Ca variability of *N. pachyderma* (s) and *G. bulloides*: Implications for seawater temperature reconstruction, *Earth Planet. Sci. Lett.*, *376*, 137–144, doi:10.1016/j.epsl.2013.06.019.

Kandiano, E. S., and H. A. Bauch (2002), Implications of planktic foraminiferal size fractions for the glacial-interglacial paleoceanography of the polar North Atlantic, *J. Foramin. Res.*, *32*, 245–251.

Kissel, C., C. Laj, L. Labeyrie, T. M. Dokken, A. Voelker, and D. Blamart (1999), Rapid climatic variations during marine isotopic stage 3: Magnetic analysis of sediments from Nordic Seas and North Atlantic, *Earth Planet. Sci. Lett.*, *171*, 489–502, doi:10.1016/S0012-821X(99)00162-4.

Knorr, G., and G. Lohmann (2007), Rapid transitions in the Atlantic thermohaline circulation triggered by global warming and meltwater during the last deglaciation, *Geochem. Geophys. Geosyst.*, *8*, Q12006, doi:10.1029/2007GC001604.

Kozdon, R., T. Ushikubo, N. T. Kita, M. Spicuzza and J. W. Valley (2009), Intratest oxygen isotope variability in the planktonic foraminifer *N. pachyderma*: Real vs. apparent vital effects by ion microprobe, *Chem. Geol.*, *258*, 327–337, doi:10.1016/j.chemgeo.2008.10.032.

Lea, D. W., and E. A. Boyle (1991), Barium in planktonic foraminifera, *Geochim. Cosmochim. Acta*, *55*, 3321–3331, doi:10.1016/00167037(91)90491M.

Lévesque, L. (1995), Distribution des assemblages de coccolithes dans les sédiments récents des moyennes latitudes de l'Atlantique Nord: développement de fonctions de transfert paléocéanographiques. MS dissertation, Université du Québec a Montréal, Montréal.

Martin, P. A., and D. W. Lea (2002), A simple evaluation of cleaning procedures on fossil benthic foraminiferal Mg/Ca, *Geochem. Geophys. Geosyst.*, *3*, 1–8, doi:10.1029/2001GC000280.

Meland, M. Y., E. Jansen, H. Elderfield, T. M. Dokken, A. Olsen, and R. G. J. Bellerby (2006), Mg/Ca ratios in the planktonic foraminifer *Neogloboquadrina pachyderma* (sinistral) in the northern North Atlantic/Nordic Seas, *Geochem. Geophys. Geosyst.*, *7*, Q06P14, doi:10.1029/2005GC001078.

Meland, M. Y., T. M. Dokken, E. Jansen, and K. Hevrøy (2008), Water mass properties and exchange between the Nordic seas and the northern North Atlantic during the period 23–6 ka: Benthic oxygen isotopic evidence, *Paleoceanography*, *23*, PA1210, doi:10.1029/2007PA001416.

Mork, K. A., and J. Blindheim (2000), Variations in the Atlantic inflow to the Nordic Seas, 1955–1996, *Deep Sea Res., Part I*, *47*, 1035–1057, doi:10.1016/S0967-0637(99)00091-6.

Nürnberg, D. (1995), Magnesium in tests of *Neogloboquadrina pachyderma* sinistral from high northern and southern latitudes, *J. Foramin. Res.*, *25*, 350–368.

Nürnberg, D., J. Bijma, and C. Hemleben (1996), Assessing the reliability of magnesium in foraminiferal calcite as a proxy for water mass temperatures, *Geochim. Cosmochim. Acta*, *60*, 803–814, doi:10.1016/0016-7037(95)00446-7.

Nyland, B. F., E. Jansen, H. Elderfield, and C. Andersson (2006), *Neogloboquadrina pachyderma* (dex. and sin.) Mg/Ca and $\delta^{18}O$ records from the Norwegian Sea, *Geochem. Geophys. Geosyst.*, *7*, Q10P17, doi:10.1029/2005GC001055.

Orvik, K. A., and P. Niiler (2002), Major pathways of Atlantic water in the northern North Atlantic and Nordic Seas toward Arctic, *Geophys. Res. Lett.*, *29*(19), 1896, doi:10.1029/2002GL015002.

Pena, L. D., E. Calvo, I. Cacho, S. Eggins, and C. Pelejero (2005), Identification and removal of Mn-Mg-rich contaminant phases on foraminiferal tests: Implications for Mg/Ca past temperature reconstructions, *Geochem. Geophys. Geosyst.*, *6*, Q09P02, doi:10.1029/2005GC000930.

Petersen, S. V., D. P., Schrag, and P. U. Clark (2013), A new mechanism for Dansgaard-Oeschger cycles, *Paleoceanography*, *28*, 24–30, doi:10.1029/2012PA002364.

Pflaumann, U., et al. (2003), Glacial North Atlantic: Sea-surface conditions reconstructed by GLAMAP 2000, *Paleoceanography 18*(3), 1065, doi:10.1029/2002PA000774.

Rahmstorf, S., J. E. Box, G. Feulner, M. E. Mann, A. Robinson, S. Rutherford, and E. J. Schaffernicht (2015), Exceptional twentieth-century slowdown in Atlantic Ocean overturning circulation, *Nat. Clim. Change*, *5*, 475–480, doi:10.1038/NCLIMATE2554.

Rasmussen, S. O., et al. (2014), A stratigraphic framework for abrupt climatic changes during the Last Glacial period based on three synchronized Greenland ice-core records: Refining and extending the INTIMATE event stratigraphy, *Quat. Sci. Rev.*, *106*, 14–28, doi:10.1016/j.quascirev.2014.09.007.

Rasmussen, T. L., and E. Thomsen (2004), The role of the North Atlantic Drift in the millennial timescale glacial climate fluctuations, *Palaeogeogr. Palaeoclim. Palaeoecol.*, *210*, 101–116, doi:10.1016/j.palaeo.2004.04.005.

Rasmussen, T. L., E. Thomsen, L. Labeyrie, and T. C. E. van Weering (1996), Circulation changes in the Faeroe-Shetland Channel correlating with cold events during the last glacial period (58–10 ka), *Geology*, *24*, 937–940, doi:10.1130/0091-7613(1996)024 < 0937:ccitfs>2.3.co;2.

Rasmussen, T. L., E. Balbon, E. Thomsen, L. Labeyrie, and T. C. E. Van Weering (1999), Climate records and changes in deep outflow from the Norwegian Sea ~150–55 ka, *Terra Nova*, *11*, 61–66, doi:10.1046/j.1365-3121.1999.00226.x.

Rasmussen, T. L., E. Thomsen, A. Kuijpers, and S. Wastegård (2003a), Late warming and early cooling of the sea surface in the Nordic seas during MIS 5e (Eemian Interglacial), *Quat. Sci. Rev.*, *22*, 809–821, doi:10.1016/S0277-3791(02)00254-8.

Rasmussen, T. L., D. W. Oppo, E. Thomsen, and S. J. Lehman (2003b), Deep sea records from the southeast Labrador Sea: Ocean circulation changes and ice-rafting events during the last 160,000 years, *Paleoceanography*, *18*(1), 1018, doi:10.1029/2001PA000736.

Regenberg, M., D. Nürnberg, S. Steph, J. Groeneveld, D. Garbe-Schönberg, R. Tiedemann, and W.-C. Dullo (2006), Assessing the effect of dissolution on planktonic foraminiferal Mg/Ca ratios: Evidence from Caribbean core tops, *Geochem. Geophys. Geosyst.*, *7*, Q07P15, doi: 10.1029/2005GC001019.

Risebrobakken, B., T. Dokken, O. H. Otterå, E. Jansen, Y. Gao, and H. Drange (2007), Inception of the Northern European ice sheet due to contrasting ocean and insolation forcing, *Quat. Res.*, *67*, 128–135.

Rosell-Melé, A., and P. Comes (1999), Evidence for a warm last glacial maximum in the Nordic Seas, or an example of shortcomings in UK $37'$ and UK 37 to estimate low sea surface temperature?, *Paleoceanography*, *14*, 770–776.

Rosenthal, Y., et al. (2004), Interlaboratory comparison study of Mg/Ca and Sr/Ca measurements in planktonic foraminifera for paleoceanographic research, *Geochem. Geophys. Geosyst.*, *5*, Q04D09, doi:10.1029/2003GC000650.

Ruddiman, W. F., A. McIntyre, V. Niebler-Hunt, and J. T. Durazzi (1980), Oceanic evidence for the mechanism of rapid Northern Hemisphere glaciation, *Quat. Res.*, *13*, 33–64.

Russell, A. D., B. Hönisch, H. J. Spero, and D. W. Lea (2004), Effects of seawater carbonate ion concentration and temperature on shell U, Mg, and Sr in cultured planktonic foraminifera, *Geochim. Cosmochim. Acta*, *68*, 4347–4361, doi:10.1016/j.gca.2004.03.013.

Seierstad, I. K., et al. (2014), Consistently dated records from the Greenland GRIP, GISP2 and NGRIP ice cores for the past 104 ka reveal regional millennial-scale δ^{18}O gradients with possible Heinrich event imprint, *Quat. Sci. Rev.*, *106*, 29–46, doi:10.1016/j.quascirev.2014.10.032.

Shackleton, N. J. (1967), Oxygen isotope analyses and pleistocene temperatures re-assessed, *Nature*, *215*, 15–17.

Shackleton, N. J. (1974), Attainment of isotopic equilibrium between ocean water and the benthic foraminifera genus Uvigerina: Isotopic changes in the ocean during the last glacial, in *Méthodes quantitatives d'étude des variations du climat au cours du Pléistocène*, edited by J. Labeyrie, pp. 203–209, Editions du C.N.R.S., France.

Simstich, J., M. Sarnthein, and H. Erlenkeuser (2003), Paired δ^{18}O signals of *Neogloboquadrina pachyderma* (s) and *Turborotalita quinqueloba* show thermal stratification structure in Nordic Seas, *Mar. Micropaleontol.*, *48*, 107–125, doi:10.1016/S0377-8398(02)00165-2.

Spero, H. J., J. Bijma, D. W. Lea, and B. E. Bemis (1997), Effect of seawater carbonate concentration on foraminiferal carbon and oxygen isotopes, *Nature*, *390*, 497–500.

Spero, H. J., S. Eggins, A. D. Russell, L. Vetter, M. R. Kilburn, and B. Hönisch (2015), Timing and mechanism for intratest Mg/Ca variability in a living planktic foraminifer, *Earth Planet. Sci. Lett.*, *409*, 32–42.

Stanford, J. D., E. J. Rohling, S. Bacon, A. P. Roberts, F. E. Grousset, and M. Bolshaw (2011), A new concept for the paleoceanographic evolution of Heinrich event 1 in the North Atlantic, *Quat. Sci. Rev.*, *30*, 1047–1066.

Thornalley, D. J. R., H. Elderfield, and I. N. McCave (2009), Holocene oscillations in temperature and salinity of the surface subpolar North Atlantic, *Nature*, *457*, 711–714.

Thornalley, D. J., I. N. McCave, and H. Elderfield (2010), Freshwater input and abrupt deglacial climate change in the North Atlantic, *Paleoceanography*, *25*, PA1201, doi:10.1029/2009PA001772.

Thornalley, D. J. R., H. Elderfield, and I. N. McCave (2011), Reconstructing North Atlantic deglacial surface hydrography and its link to the Atlantic overturning circulation, *Global Planet. Change*, *79*, 163–175, doi:10.1016/j.gloplacha.2010.06.003.

Van Nieuwenhove, N., H. A. Bauch, F. Eynaud, E. Kandiano, E. Cortijo, and J.-L. Turon (2011), Evidence for delayed poleward expansion of North Atlantic surface waters during the last interglacial (MIS 5e), *Quat. Sci. Rev.*, *30*, 934–946, doi:10.1016/j.quascirev.2011.01.013.

Van Nieuwenhove, N., H. A. Bauch, and H. Andruleit (2013), Multiproxy fossil comparison reveals contrasting surface ocean conditions in the western Iceland Sea for the last two interglacials, *Palaeogeogr. Palaeoclim. Palaeoecol.*, *370*, 247–259, doi:10.1016/j.palaeo.2012.12.018.

Waelbroeck, C., L. C. Skinner, L. Labeyrie, J.-C. Duplessy, E. Michel, N. Vazquez Riveiros, J.-M. Gherardi, and F. Dewilde (2011), The timing of deglacial circulation changes in the Atlantic, *Paleoceanography*, *26*, PA3213, doi:10.1029/2010PA002007.

Wastegård, S., T. L. Rasmussen, A. Kuijpers, T. Nielsen, and T. C. E. van Weering (2006), Composition and origin of ash zones from Marine Isotope Stages 3 and 2 in the North Atlantic, *Quat. Sci. Rev.*, *25*, 2409–2419, doi:10.1016/j.quascirev.2006.03.001.

Yu, J., H. Elderfield, and B. Hönisch (2007a), B/Ca in planktonic foraminifera as a proxy for surface seawater pH, *Paleoceanography*, *22*, PA2202, doi:10.1029/2006PA001347.

Yu, J., H. Elderfield, M. Greaves, and J. Day (2007b), Preferential dissolution of benthic foraminiferal calcite during laboratory reductive cleaning, *Geochem. Geophys. Geosyst.*, *8*, PA2202, doi:10.1029/2006GC001571.

Yu, J., D. J. R. Thornalley, J. W. B. Rae, and N. I. McCave (2013), Calibration and application of B/Ca, Cd/Ca, and δ^{11}B in *Neogloboquadrina pachyderma* (sinistral) to constrain CO_2 uptake in the subpolar North Atlantic during the last deglaciation, *Paleoceanography*, *28*, 237–252, doi:10.1002/palo.20024.